Non-linear Simulation of Edge Localized Modes in ASDEX Upgrade

Alexander Lessig,
Matthias Hölzl, François Orain, Sibylle Günter, Marina Becoulet, Guido Huysmans, Stanislas Pamela, Mike Dunne, the ASDEX Upgrade Team

IPP

ASDEX Upgrade

EUROfusion

HEPP
International Helmholtz Graduate School for Plasma Physics

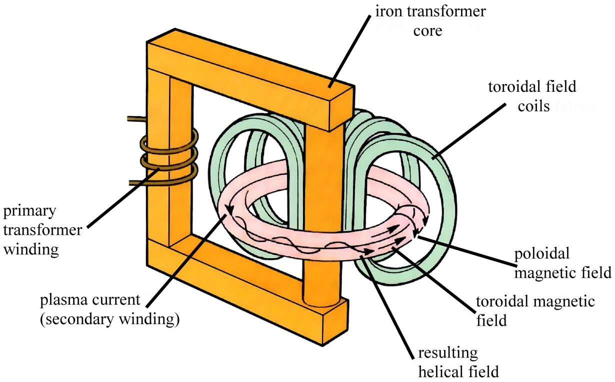

- magnetic field in toroidal direction created by toroidal field coils
- inductively driven plasma current creates poloidal magnetic field

→ plasma confinement by helically winding field lines

Edge Localized Modes

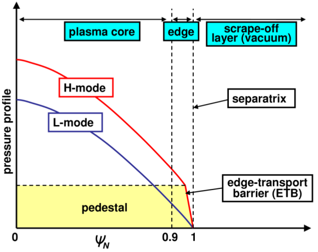

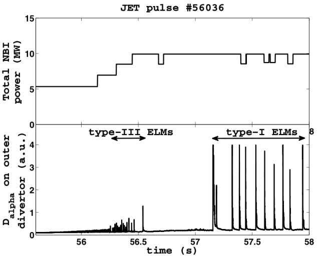

S. Pamela. Ph.D. thesis, University of Provence (2010)

- relaxation-like oscillatory instability at the boundary of H-mode plasmas (pedestal collapse)
- driven by large pressure gradients and current densities
- eject particles and energy on very short time-scales
- plasma particle and energy content decreased by up to 10%

- **high heat loads on plasma-facing components (in particular divertor targets)**

$\rightarrow$ comprehensive theoretical understanding necessary for control and prediction of ELM properties

Overview

ASDEX Upgrade IPP

- **3D Non-linear MHD in X-point tokamak geometry**

  G. Huysmans and O. Czarny. *Nucl Fusion*, 47, 659 (2007)

- European project
- multi-purpose non-linear MHD code

- **Edge Localized Modes** in
  - ASDEX Upgrade M. Hölzl, S. Günter, et al. *Phys Plasmas*, 19, 082505 (2012)
  - MAST S. J. P. Pamela, G. T. A. Huysmans, et al. *PPCF*, 55, 095001 (2013)
  - JET S. J. P. Pamela, G. T. A. Huysmans, et al. *PPCF*, 53, 054014 (2011)
  - ITER G. Huysmans and A. Loarte. *J Nucl Mater*, 438, s57 (2013)
- **Resonant Magnetic Perturbations** M. Bécoulet, F. Orain, et al. *Phys Rev Lett*, 113, 115001 (2014)
- **Pellet ELM Triggering** G. Huysmans, S. Pamela, et al. *23rd IAEA*, THS/7-1 (2010)
- **Tearing Modes** J. Pratt and E. Westerhof. 54th APS (2012)
- **Disruptions** A. Fil, E. Nardon, et al. *Phys Plasmas*, 22, 062509 (2015)
- ...

Reduced MHD

- **Starting point: resistive MHD equations** including particle and heat sources/diffusion

$$
\begin{aligned}
\partial_t \rho + \nabla \cdot (\rho \mathbf{v}) &= \nabla \cdot (D_\perp \nabla_\perp \rho) + S_\rho \\
\rho \left(\partial_t + \mathbf{v} \cdot \nabla \right) \mathbf{v} &= -\nabla p + \mathbf{j} \times \mathbf{B} + \mu \Delta \mathbf{v} \\
\partial_t p + \mathbf{v} \cdot \nabla p + \gamma p \nabla \cdot \mathbf{v} &= \nabla \cdot \left(\kappa_\parallel \nabla_\parallel T + \kappa_\perp \nabla_\perp T \right) + S_T \\
\mathbf{E} + \mathbf{v} \times \mathbf{B} &= \eta \mathbf{j} \\
\nabla \times \mathbf{E} &= -\frac{\partial \mathbf{B}}{\partial t} \\
\nabla \times \mathbf{B} &= \mu_0 \mathbf{j} \\
\nabla \cdot \mathbf{B} &= 0
\end{aligned}
$$

- Variables: ρ, $\mathbf{v}$, p, $\mathbf{B}$ with $p = R_s \rho T$

Reduced MHD

- Definition of magnetic and velocity vector fields: $\mathbf{B} := \underbrace{\frac{F_0}{R}\mathbf{e}_\phi}_{\mathbf{B}_\phi} + \underbrace{\frac{1}{R}\nabla\Psi \times \mathbf{e}_\phi}_{\mathbf{B}_{\text{pol}}}$

  and $\mathbf{v} := \underbrace{-R\nabla u \times \mathbf{e}_\phi}_{\mathbf{v}_\perp} + \underbrace{v_{||}\mathbf{B}}_{\mathbf{v}_{||}}$ with $|\mathbf{B}_\phi| \gg |\mathbf{B}_{\text{pol}}|$

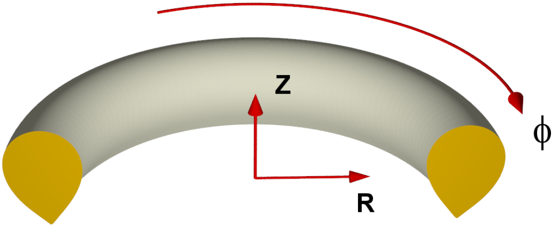

Reduced MHD

ASDEX Upgrade IPP

- Definition of magnetic and velocity vector fields: $\mathbf{B} := \underbrace{\frac{F_0}{R}\mathbf{e}_\phi}_{\mathbf{B}_\phi} + \underbrace{\frac{1}{R}\nabla\Psi \times \mathbf{e}_\phi}_{\mathbf{B}_{\text{pol}}}$

and $\mathbf{v} := \underbrace{-R\nabla u \times \mathbf{e}_\phi}_{\mathbf{v}_\perp} + \underbrace{v_{||}\mathbf{B}}_{\mathbf{v}_{||}}$ with $|\mathbf{B}_\phi| \gg |\mathbf{B}_{\text{pol}}|$

$$\partial_t \rho + \nabla\cdot(\rho\mathbf{v}) = \nabla\cdot(D_\perp\nabla_\perp\rho) + S_\rho$$

$$\mathbf{e}_\phi\cdot\nabla\times R^2\left\{\rho\left(\partial_t + \mathbf{v}\cdot\nabla\right)\mathbf{v} = -\nabla p + \mathbf{j}\times\mathbf{B} + \mu\Delta\mathbf{v}\right\}$$

$$\mathbf{B}\cdot\left\{\rho\left(\partial_t + \mathbf{v}\cdot\nabla\right)\mathbf{v} = -\nabla p + \mathbf{j}\times\mathbf{B} + \mu\Delta\mathbf{v}\right\}$$

$$\partial_t p + \mathbf{v}\cdot\nabla p + \gamma p\nabla\cdot\mathbf{v} = \nabla\cdot\left(\kappa_{||}\nabla_{||}T + \kappa_\perp\nabla_\perp T\right) + S_T$$

$$\partial_t\Psi = R[\Psi, u] + \frac{\eta}{\mu_0}j - F_0\partial_\phi u$$

- Definitions: $\omega := \nabla_\perp^2 u$ and $j := \Delta^*\Psi$
- Variables: $\rho, \omega, u, v_{||}, p, \Psi, j$ with $p = R_s\rho T$

E. Frank, M. Hölzl, A. Lessig, and E. Sonnendrücker. *ESAIM Math Model Numer Anal*, 49, 1331 (2015)

Discretization

- **toroidal direction:** Fourier decomposition
- **poloidal plane:** 2D Bezier finite elements (C^1, iso-parametric)

$$\mathbf{P}(s,t) = \sum_{i=0}^{3} \sum_{j=0}^{3} \mathbf{P}_{ij} B_i^3(s) B_j^3(t)$$

$$B_0^3(s) = (1-s)^3$$
$$B_1^3(s) = 3(1-s)^2 s$$
$$B_2^3(s) = 3(1-s)s^2$$
$$B_3^3(s) = s^3$$

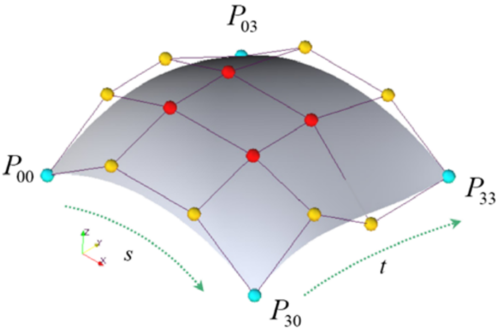

O. Czarny and G. Huysmans. *J Comput Phys*, 227, 7423 (2008)

Typical Simulation

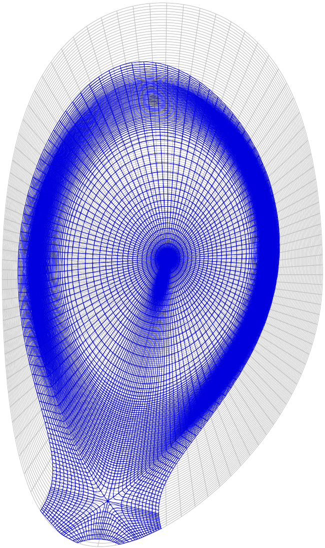

- Construction of polar grid
- Solution of Grad-Shafranov equation on polar grid using input profiles
  (F_0, Ψ_{bnd}, profiles for T, ρ, FF')
- Construction of flux-aligned X-point grid
- ideal Wall and Bohm boundary conditions
- Fully implicit time integration
  (GMRES, Physics-based preconditioner, hybrid openMP/MPI parallelization)
- Postprocessing

Full Crash Simulation

- ASDEX Upgrade discharge #29342@4.25s **CLISTE reconstruction by Mike Dunne**
- toroidal modes $n = 0 \ldots 22$ included
- core resistivity in ASDEX Upgrade: $\sim 1 \cdot 10^{-8} \Omega m$
- core resistivity in simulation: $2.5 \cdot 10^{-7} \Omega m$
- about 500,000 cpu-hours on Helios

Modelling

Energy Time-Trace

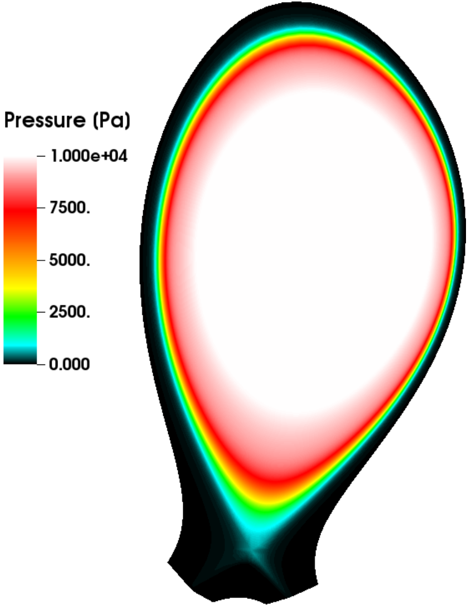

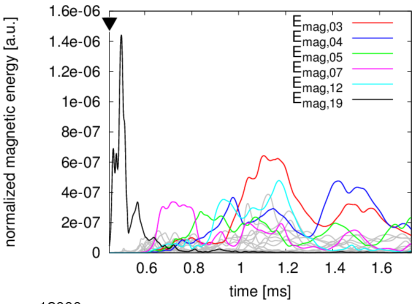

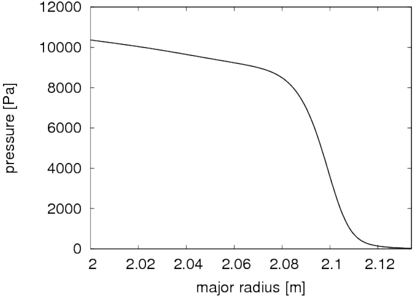

Energy Time-Trace

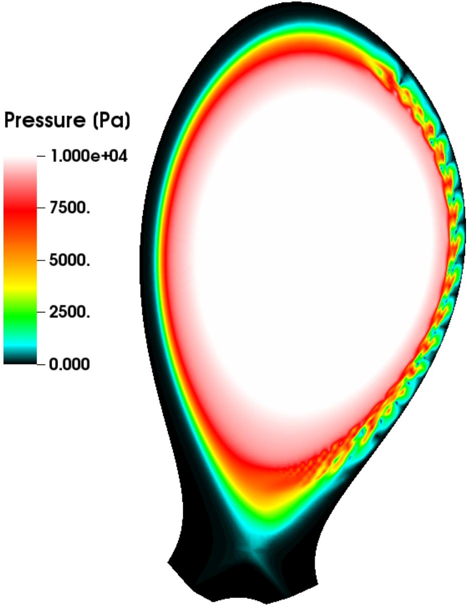

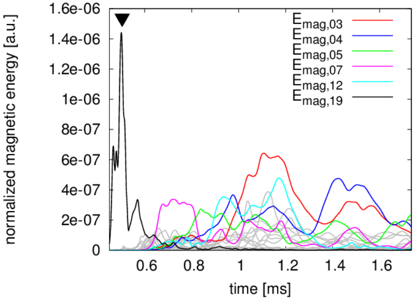

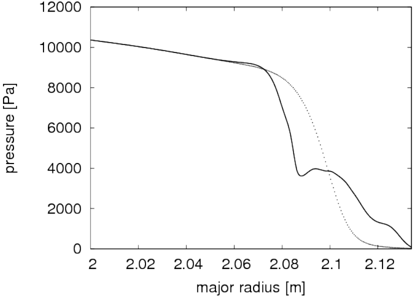

Energy Time-Trace

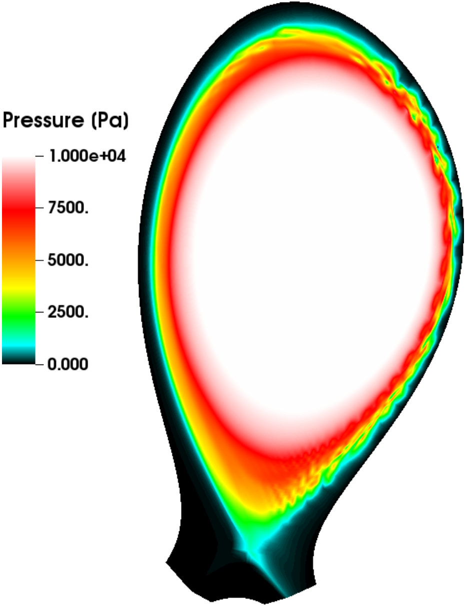

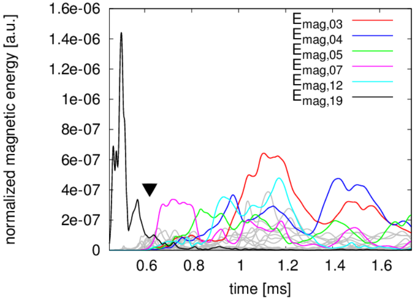

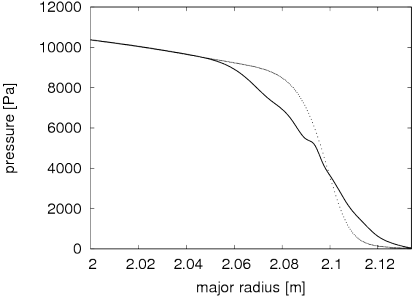

Energy Time-Trace

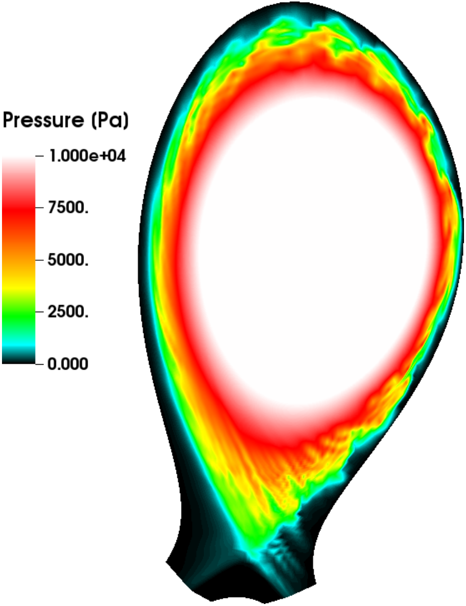

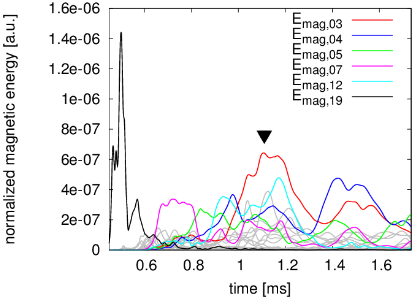

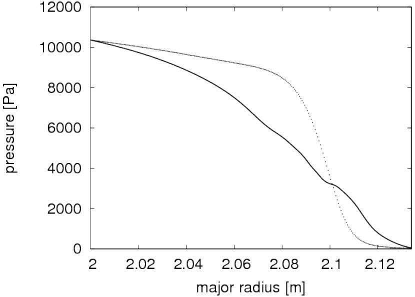

Resolution Scan

ASDEX Upgrade

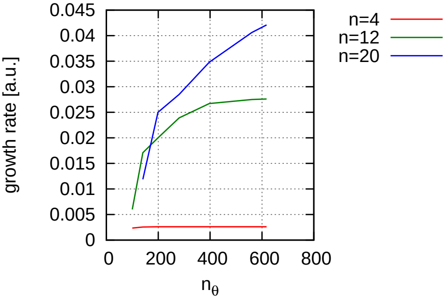

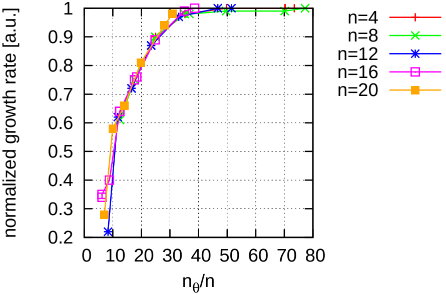

- ASDEX Upgrade discharge #31128
- core resistivity in simulation: $2.5 \cdot 10^{-7}\,\Omega\mathrm{m}$ (AUG: $\sim 1 \cdot 10^{-8}\,\Omega\mathrm{m}$)
- high-n components require high grid resolution $(m = q \cdot n)$ $\rightarrow$ **linearly not fully resolved**

Modelling   Resolution Scan

ASDEX Upgrade

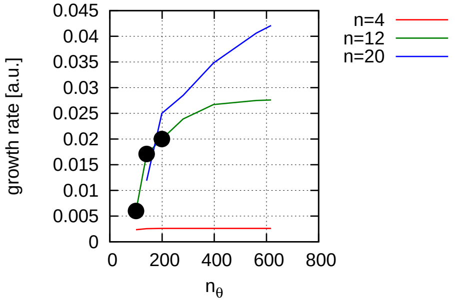

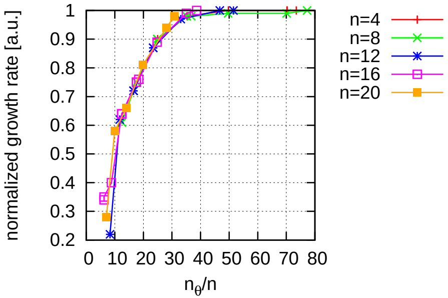

- ASDEX Upgrade discharge #31128
- core resistivity in simulation: $2.5 \cdot 10^{-7}\Omega\mathrm{m}$ (AUG: $\sim 1 \cdot 10^{-8}\Omega\mathrm{m}$)
- high-n components require high grid resolution $(m = q \cdot n)$ $\rightarrow$ **linearly not fully resolved**

Resolution Scan

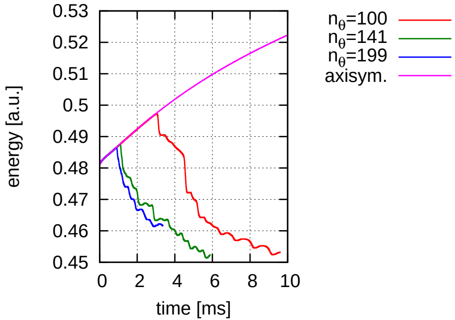

- ASDEX Upgrade discharge #31128
- core resistivity in simulation: $2.5 \cdot 10^{-7} \Omega \mathrm{m}$ (AUG: $\sim 1 \cdot 10^{-8} \Omega \mathrm{m}$)
- high-n components require high grid resolution $(m = q \cdot n) \rightarrow$ **linearly not fully resolved**
- losses converged $\rightarrow$ **non-linearly well resolved**

Losses/Divertor Heat Load

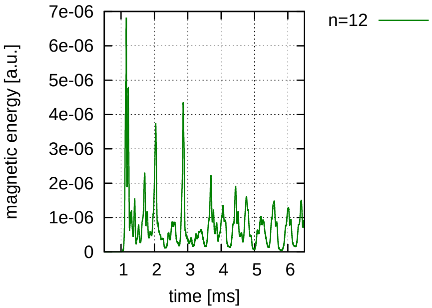

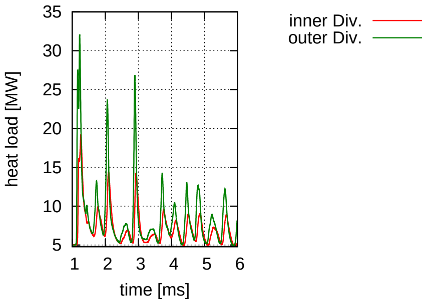

- main ELM phase for $t \leqslant 3$ms
- ballooning turbulence for $t > 3$ms
- particle/energy losses of $\sim 10\%$
- asymmetry in divertor heat load
- diamagnetic drift influences heat load asymmetry and ballooning turbulence

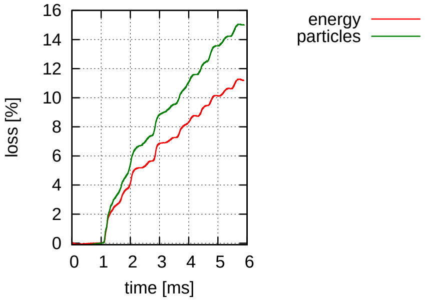

F. Orain, M. Becoulet, et al. *Phys Rev Lett*, 114, 035001 (2015)

Filament Dynamics

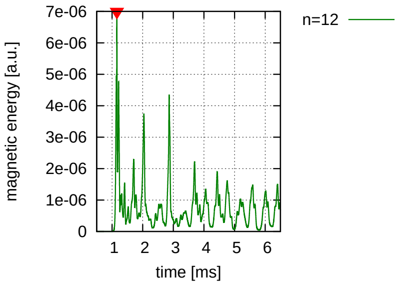

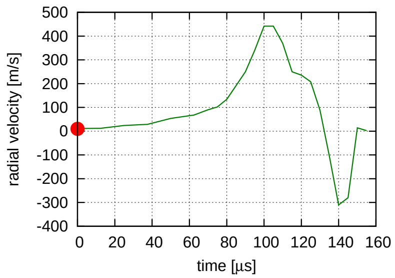

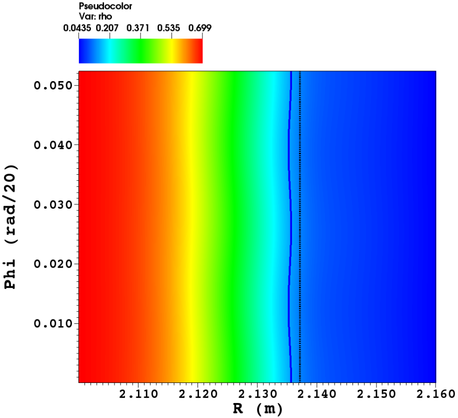

- radial size of filament: ∼ 4cm
- poloidal size of filament: ∼ 13.5cm

Filament Dynamics

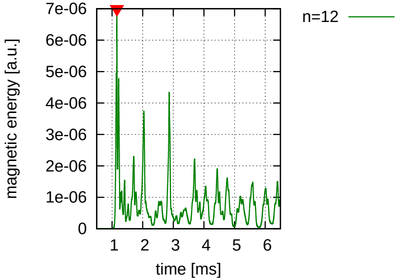

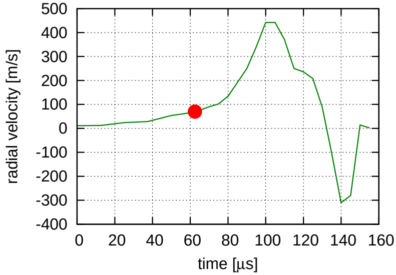

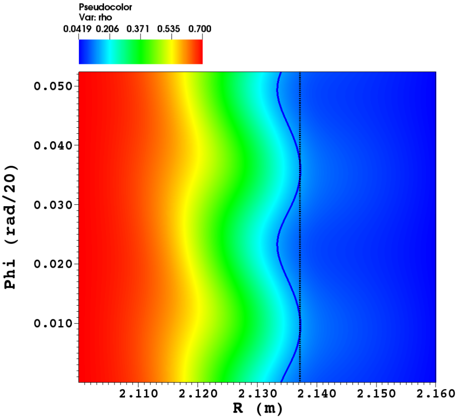

- radial size of filament: ∼ 4cm
- poloidal size of filament: ∼ 13.5cm

Filament Dynamics

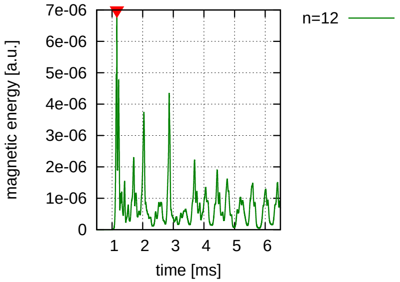

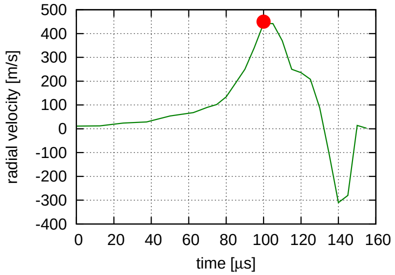

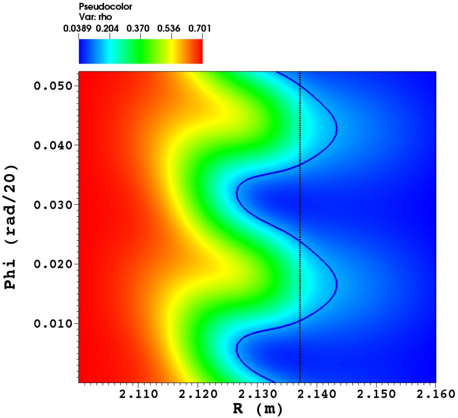

- radial size of filament: ~ 4cm
- poloidal size of filament: ~ 13.5cm

Modelling Filament Dynamics

ASDEX Upgrade

IPP

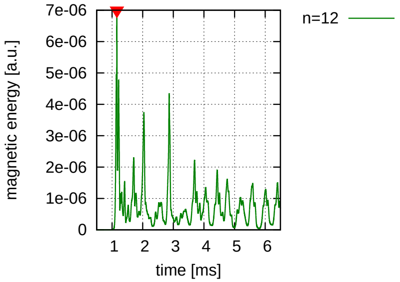

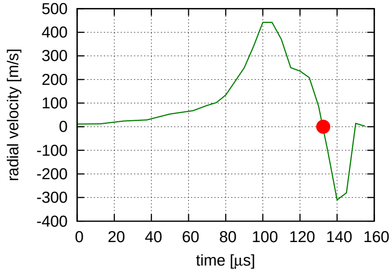

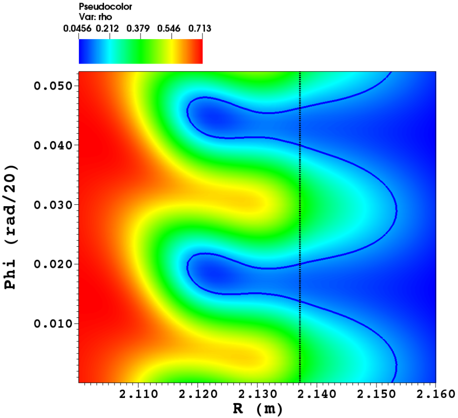

- radial size of filament: ∼ 4cm
- poloidal size of filament: ∼ 13.5cm

Filament Dynamics

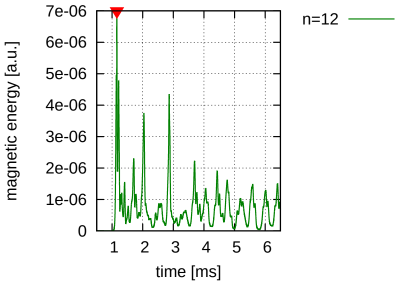

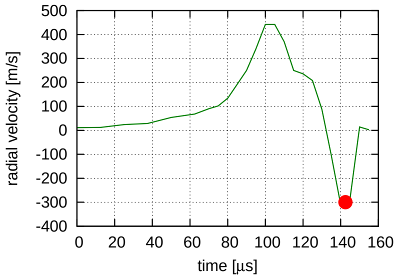

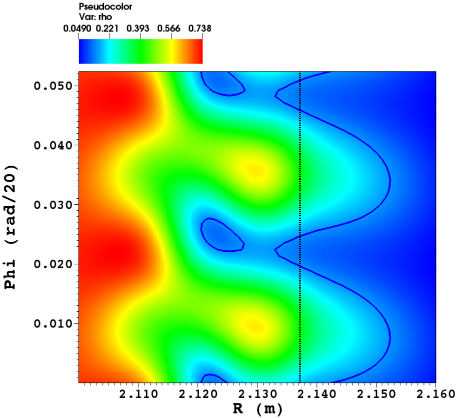

- radial size of filament: ∼ 4cm
- poloidal size of filament: ∼ 13.5cm

Filament Dynamics

ASDEX Upgrade

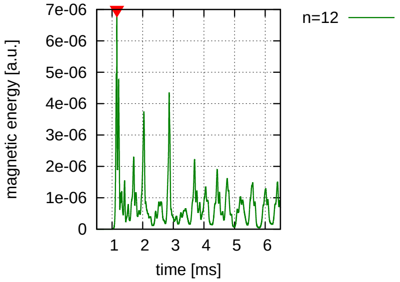

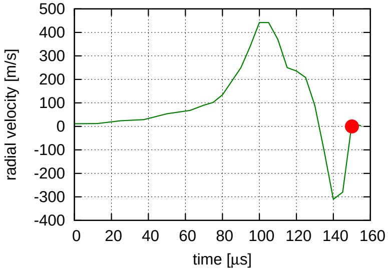

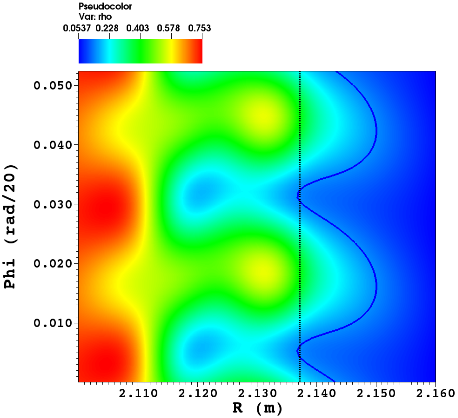

- radial size of filament: $\sim$ 4cm
- poloidal size of filament: $\sim$ 13.5cm

Filament Dynamics

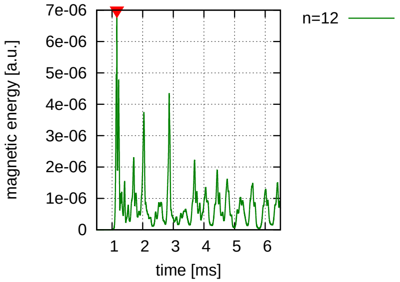

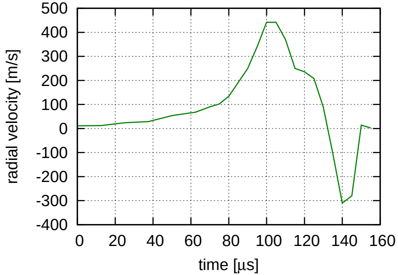

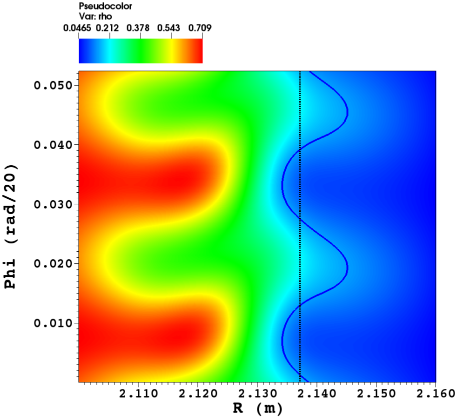

- radial size of filament: ∼ 4cm
- poloidal size of filament: ∼ 13.5cm

Summary and Outlook

Summary

- high-n components require high grid resolution → computational limits in linear phase/non-linearly well resolved
- ELM losses comparable to experimental observations for type-I ELMs

  H. Zohm. *PPCF*, 38, 105 (1996)
- evolution of toroidal Fourier spectrum and pedestal in qualitative agreement with experimental observations

  R. P. Wenninger, H. Reimerdes, O. Sauter, and H. Zohm. *Nucl Fusion*, 53, 113004 (2013)

  P. Schneider, E. Wolfrum, et al. *PPCF*, 56, 025011 (2014)

Outlook

- include diamagnetic drifts (act stabilizing on high mode numbers)
- include toroidal rotation and neoclassical viscosity
- identify different ELM types in our simulations as observed in experiments
- further comparison to experimental observations, e.g. pedestal evolution and heat deposition patterns

References

M. Bécoulet, F. Orain, et al. *Phys Rev Lett*, 113, 115001 (2014).

O. Czarny and G. Huysmans. *J Comput Phys*, 227, 7423 (2008).

A. Fil, E. Nardon, et al. *Phys Plasmas*, 22, 062509 (2015).

E. Frank, M. Hölzl, A. Lessig, and E. Sonnendrücker. *ESAIM Math Model Numer Anal*, 49, 1331 (2015).

M. Hölzl, S. Günter, et al. *Phys Plasmas*, 19, 082505 (2012).

G. Huysmans and O. Czarny. *Nucl Fusion*, 47, 659 (2007).

G. Huysmans and A. Loarte. *J Nucl Mater*, 438, s57 (2013).

G. Huysmans, S. Pamela, et al. *23rd IAEA*, THS/7-1 (2010).

F. Orain, M. Becoulet, et al. *Phys Rev Lett*, 114, 035001 (2015).

S. Pamela. Ph.D. thesis, University of Provence (2010).

S. J. P. Pamela, G. T. A. Huysmans, et al. *PPCF*, 53, 054014 (2011).

S. J. P. Pamela, G. T. A. Huysmans, et al. *PPCF*, 55, 095001 (2013).

J. Pratt and E. Westerhof. 54th APS (2012).

P. Schneider, E. Wolfrum, et al. *PPCF*, 56, 025011 (2014).

R. P. Wenninger, H. Reimerdes, O. Sauter, and H. Zohm. *Nucl Fusion*, 53, 113004 (2013).

H. Zohm. *PPCF*, 38, 105 (1996).

This work has been carried out within the framework of the EUROfusion Consortium and has received funding from the Euratom research and training programme 2014-2018 under grant agreement number 633053. The views and opinions expressed herein do not necessarily reflect those of the European Commission.

Diamagnetic Stabilization

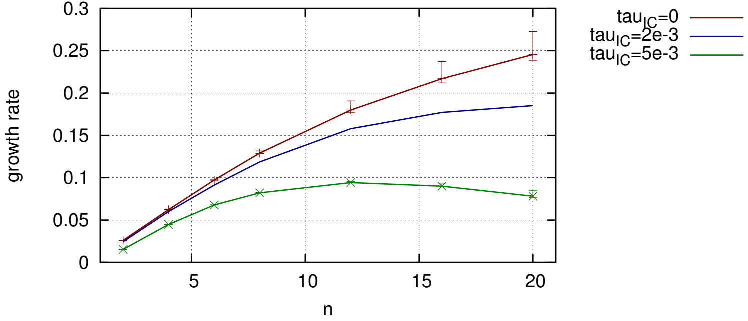

- diamagnetic drift terms stabilize high-n components
- intermediate mode numbers become dominant